

# Pressure-induced phase transformation of BaS: An *ab initio* constant pressure study

Murat Durandurdu \*

Department of Physics, University of Texas at El Paso, El Paso, TX 79968, USA  
Fizik Bölümü, Ahi Evran Üniversitesi, Kırşehir 40100, Turkey

## ARTICLE INFO

### Article history:

Received 10 August 2009

In final form 28 October 2009

Available online 1 November 2009

### Keywords:

Phase transformation

*Ab initio*

Semiconductor

## ABSTRACT

We present an *ab initio* molecular dynamics study of pressure-induced structural phase transition in BaS. We successfully observe the NaCl-to-CsCl phase transformation through the simulations. We also determine the transformation mechanism of this simple phase transformation and compare it with the previously proposed mechanisms.

© 2009 Elsevier B.V. All rights reserved.

## 1. Introduction

The barium chalcogenide compounds BaX ( $X = S, Se$  and  $Te$ ) are technologically important materials having a wide range applications in microelectronics, light-emitting diodes, laser diodes, and magneto-optical devices. These materials are simplest and most typical ionic systems and they crystallize in NaCl-type (B1) structure at ambient conditions. Understanding pressure-induced phase transformations of these materials as well as their mechanical and electronic properties is of great importance. With the application of pressure, they undergo a first-order structural phase transition to CsCl (B2) structure [1–3]. To our knowledge, no molecular dynamics simulation has been applied to study their pressure-induced phase transformations. In this study, we carry out constant pressure *ab initio* molecular dynamics simulations to fully explain the microscopic nature of the pressure-induced phase transition of BaS. Our findings demonstrate that the B1-to-B2 phase change follows the Buerger mechanism [4] but the intermediate phases formed during the phase transformation are different from the previously proposed intermediate phases [5–7].

## 2. Method

All calculations were performed using the SIESTA code [8], which is based on the first principles pseudopotential method within DFT. For the Kohn–Sham Hamiltonian, the generalized-gradient approximation (GGA) for the exchange correlation functional of Perdew et al. [9] was chosen with norm conserving pseudopo-

tentials of Troullier–Martin type [10]. A double-zeta plus polarization numerical basis set was selected together with a real-space mesh cutoff corresponding to upper energy cutoff 150.0 Ry. The simulation cell consists of 64 atoms with periodic boundary conditions. We used  $\Gamma$ -point sampling for the Brillouin zone integration, which is reasonable for a simulation cell with 64-atoms since the energy difference between the 64 atoms simulation cell with only  $\Gamma$  point and the 2-atoms primitive cell with 256- $k$  points (see below) is less than about 0.03 eV/atom. The molecular dynamics (MD) simulations were performed using the NPH (constant number of atoms, constant pressure, and constant enthalpy) ensemble. The reason for choosing this ensemble is to remove the thermal fluctuation, which facilitates easier examination of the structure during the phase transformation. Pressure was applied via the method of Parrinello and Rahman [11]. The system was first equilibrated at zero pressure, and then pressure was gradually increased by an increment of 100.0 GPa. The equilibration period is 1000 time step with a time step of 1 fs. We also used the power quenching technique during the MD simulations. In this technique, each velocity component is quenched individually. At each time step, if the force and velocity components have opposite sign, the velocity component is set equal to zero. All atoms or supercell velocities (for cell shape optimizations) are then allowed to accelerate at the next time step. For the energy volume calculations, we considered the primitive cell of both B1 and B2-type phases. The Brillouin zone integration was performed with automatically generated  $10 \times 10 \times 10$   $k$ -point mesh for both phases following the convention of Monkhorst and Pack [12].

In order to determine the intermediate state during the phase transformation, we used the KPLOT program [13] that provides detailed information about space group, cell parameters and atomic position of a given structure. For the symmetry analysis we used

\* Address: Department of Physics, University of Texas at El Paso, El Paso, TX 79968, USA.

E-mail address: [mdurandurdu@utep.edu](mailto:mdurandurdu@utep.edu)

0.2 Å, 4°, and 0.7 Å tolerances for bond lengths, bond angles and interplanar spacing, respectively.

### 3. Results

In order to determine the ground states properties of BaS, the total energies of B1 and B2 phases are calculated in for different volumes and fitted to the third order Birch Murnagham equation of state (EOS). The energy–volume data is given in Fig. 1. From the EOS, we determine the ground state properties such as the equilibrium lattice constant  $a$ , the bulk modulus  $B_0$  and its pressure derivative  $B'_0$ . The calculated equilibrium parameters of both phases, together with available experimental and theoretical data, are given in Table 1. Overall we find that our results are comparable with experimental and previous theoretical data [2,14–18].

In order to determine the transition pressure at  $T = 0$  K, we calculate the enthalpy,  $H = E + PV$ . The stable structure at a given pressure is the state for which the enthalpy has its lowest value and the transition pressure is calculated at which the enthalpies for the two phases are equal. Fig. 2 shows the enthalpy curves of both B1 and B2 phases. Our predicted transition pressure is 6.62 GPa, which is in excellent agreement with the experimental transition

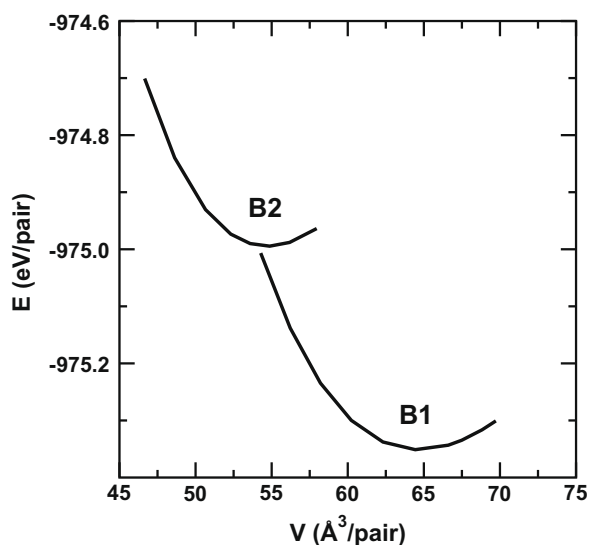


Fig. 1. The computed energies of B1 and B2 phases as a function of volume.

Table 1

Lattice parameter, bulk modulus  $B_0$ , its pressure derivative  $B'_0$  for the B1 and B2 phases of BaS and the transition pressure  $P_t$  (GPa) for the B1-to-B2 phase transformation. Refs. [2,18] are the experimental data.

Phase	$a$ (Å)	$B_0$ (GPa)	$B'_0$	$P_t$ (GPa)	Reference
B1	6.41	47.32	4.75	6.62	This study
	6.316	53.32	4.30	6.51	[14]
	6.469	42.36	5.81		[14]
	6.196	52.46		6.02	[15]
	6.46	40.25	4.16	7.03	[16]
	6.27	52.39	4.92	6.48	[17]
	6.389	39.42		6.5	[18]
		$55.1 \pm 1.4$	5.5	6.5	[2]
B2	3.72	58.03	4.78		This study
	3.874	49.5	4.48		[14]
	3.85	45.25	4.38		[14]
	3.85	43.60	4.12		[16]
	3.706	60.84			[15]
	3.76	57.27	4.24		[17]
		34.02			[18]
		$24.1 \pm 0.3$	$7.8 \pm 0.1$		[2]

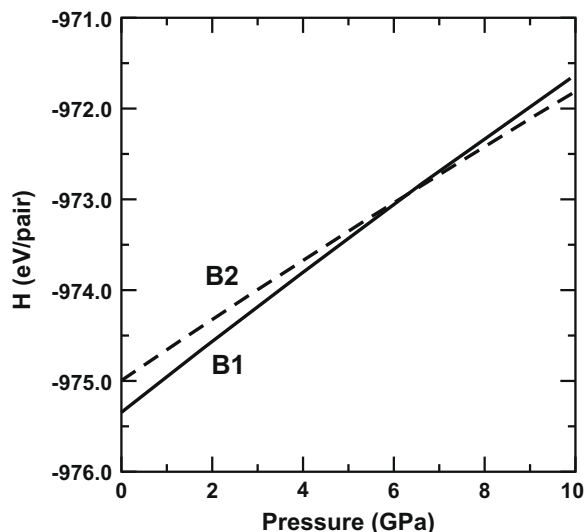


Fig. 2. The calculated enthalpies of B1 and B2 structures as a function of pressure.

pressure of 6.5 GPa and the other theoretical results of 6.02–7.03 GPa.

These findings demonstrate that the parameters used in the simulation are good enough to produce reasonable results for BaS and hence they can be safely used to explore this phase transformation using a constant pressure molecular dynamics simulations.

Fig. 3 shows the pressure-dependence of the volume determined in the MD simulations. The volume gradually decreases up to 40 GPa, at which point it dramatically decreases, indicating a first-order phase transformation. At this pressure the B1 structure transformed into B2, in agreement with experiments. The critical pressure, 30–40 GPa, predicted in MD simulation, however, considerably larger than the experimental transition pressure of 6.5 GPa. Such an overestimation in the MD simulation, analogous to superheating in MD simulations, is anticipated when the simulation conditions are considered [19]. The limited box size, the use of periodic boundary conditions and the lack of defects in the simulated structure affect the critical stress predicted in constant pressure simulations. The periodic boundary conditions lead to an

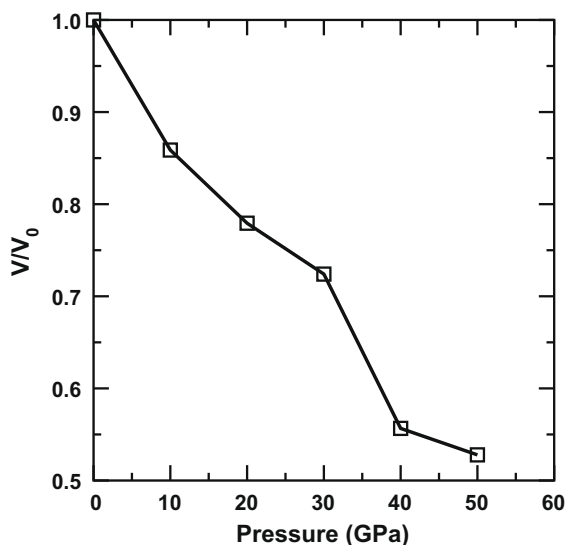


Fig. 3. The pressure–volume curve from the constant pressure *ab initio* simulation.

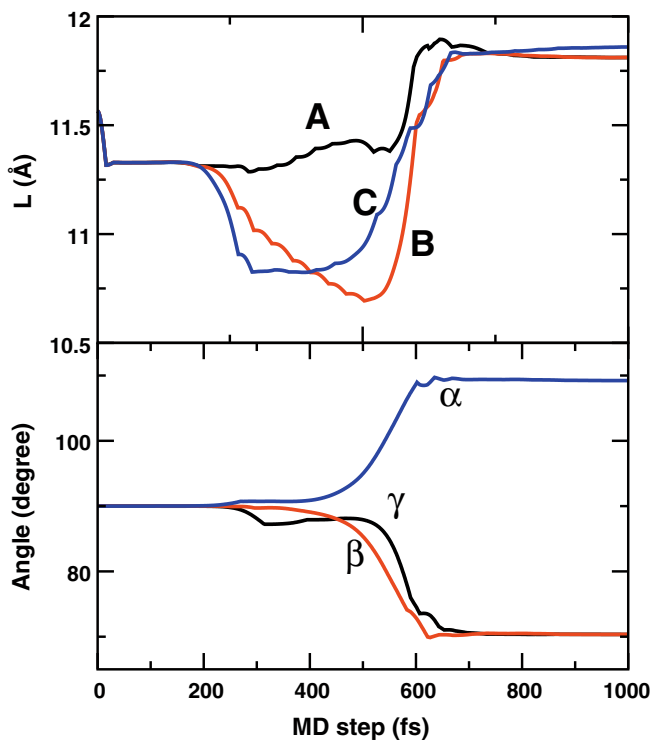


Fig. 4. Changes the simulation cell lengths and angles as a function of MD time step at 40 GPa.

additional coupling of the ions in the simulation box. The lack of any defect in the simulated structure suppresses nucleation and growing. These tend to favor a phase change, in which the whole system undergoes the phase transformation as a collective movement of all ions. As a result, systems have to cross a significant energy barrier to transform from one phase to another one. On the other hand, the thermodynamic theorem does not take into account the possible existence of such an activation barrier separating the two structural phases and hence the transition pressure predicted from MD and enthalpy calculations are significantly different from each other.

In the simulations, we can easily track the transformation mechanism of this phase change by simply analyzing the modification of the simulation cell vectors and the motion of the atomic coordinates. Fig. 4 shows the simulation cell lengths and angles as a function of the MD time step, in which A, B and C simulation cell vectors are along the [001], [010] and [001] directions, respectively. The magnitude of these vectors is plotted in the figure. As clearly seen from the figure, around 200 fs, the structure is compressed along the [010] and [001] directions and then it undergoes a shear deformation, the simulation cell angles  $\gamma$  (between A and B vectors)  $\beta$  (between A and C vectors) decrease to  $70^\circ$  while the  $\alpha$  (between A and C vectors) increases to about  $110^\circ$ . This modification is simply equivalent to the Buerger mechanism and similar to what has been observed in a MD simulation in which the B1-to-B2 phase transition of NaCl was produced at a transition pressure of about 30 GPa, close to the experimental value of 30 GPa [20]. The structural analysis suggests multiple intermediate phases for the B1-to-B2 phase transformation of BaS. Around 240 fs, we determine a tetragonal phase within  $P42/mcm$  having lattice parameters  $a = b = 5.61 \text{ \AA}$  and  $c = 5.49 \text{ \AA}$ . At 290 fs, a monoclinic phase with space group  $P_2$  forms, whose lattice parameters are  $a = 5.52 \text{ \AA}$ ,  $b = 5.64 \text{ \AA}$ ,  $5.41 \text{ \AA}$  and the monoclinic angle is  $91.35^\circ$ . Around 500 fs,  $P_2$  triclinic state with  $a = 5.36 \text{ \AA}$ ,

$b = 5.44 \text{ \AA}$ ,  $c = 5.71 \text{ \AA}$ ,  $\alpha = 92.9^\circ$ ,  $\beta = 93.15^\circ$ , and  $\gamma = 91.88^\circ$  forms. At later time steps, all angles of this triclinic phase has a tendency to increase to  $110^\circ$  but the increase in  $\alpha$  and  $\beta$  angles is faster than the other one.

The transformation mechanism observed for BaS is similar to the Buerger mechanism but the phase transformation follows several intermediate phases, which are different from the rhombohedral intermediate phase. Indeed, Zhang and Chen [21] proposed four different pathways with multiple intermediate phases for KCl. The intermediate states are different along the four pathways but the simulations indicate that the essence of phase transition is reflected by a Buerger mechanism [21]. The B1-to-B2 phase change indeed is a reconstructive phase transformation and involves large atomic displacements. Therefore, the system can transform from one phase to another by passing through various closely related paths during the transition. In other word, the transformation mechanism might follow various transition pathways or involve several intermediate states.

#### 4. Conclusions

The pressure-induced phase transformation of BaS is investigated using *ab initio* constant pressure molecular dynamics simulation. Our finding indicates that the B1-to-B2 phase transformation follows the Buerger mechanism and involves several intermediate phases. This phase transformation is also studied from the total-energy calculations. Our transition pressure and bulk properties are in good agreement with experimental and previous theoretical data.

#### Acknowledgements

The visit of the author to Ahi Evran Üniversitesi was facilitated by the Scientific and Technical Research Council of Turkey (TÜBİTAK) BİDEB-2221. The calculations were run on Sacagawea, a 128 processor Beowulf cluster, at the University of Texas at El Paso.

#### References

- [1] S.T. Weir, Y.K. Vohra, A.L. Ruoff, Phys. Rev. B 35 (1987) 874.
- [2] S.T. Weir, Y.K. Vohra, A.L. Ruoff, Phys. Rev. B 33 (1986) 4221.
- [3] T.A. Grzybowski, A.L. Ruoff, Phys. Rev. Lett. 53 (1984) 489.
- [4] M. Buerger, in: R. Smoluchowski, J.E. Mayers, W.A. Weyl (Eds.), Phase Transformations in Solids, Wiley, New York, 1948, pp. 183–211.
- [5] M. Watanabe, M. Tokonami, N. Morimoto, Acta Crystallogr., Sect. A: Cryst. Phys., Diffr., Theor. Gen. Crystallogr. A33 (1977) 284.
- [6] H.T. Stokes, D.M. Hatch, Phys. Rev. B 65 (2002) 144114.
- [7] P. Tolédano, K. Knorr, L. Ehm, W. Depmeier, Phys. Rev. B 67 (2003) 144106.
- [8] P. Ordejón, E. Artacho, J.M. Soler, Phys. Rev. B 53 (1996) 10441; D. Sánchez-Portal, P. Ordejón, E. Artacho, J.M. Soler, Int. J. Quantum Chem. 65 (1997) 453.
- [9] J.P. Perdew, K. Burke, M. Ernzerhof, Phys. Rev. Lett. 77 (1996) 3865.
- [10] N. Troullier, J.L. Martins, Phys. Rev. B 43 (1991) 1993.
- [11] M. Parrinello, A. Rahman, Phys. Rev. Lett. 45 (1980) 1196.
- [12] H.J. Monkhorst, J.D. Pack, Phys. Rev. B 13 (1976) 5188.
- [13] R. Hundt, J.C. Schön, A. Hannemann, M. Jansen, J. Appl. Crystallogr. 32 (1999) 413.
- [14] A. Bouhemadou, R. Khenata, F. Zegrar, M. Sahnoun, H. Baltache, A.H. Reshak, Comput. Mater. Sci. 38 (2006) 263.
- [15] G. Kalpana, B. Palanivel, M. Rajagopalan, Phys. Rev. B 50 (1994) 12318.
- [16] R. Khenata, M. Sahnoun, H. Baltache, M. Rerat, D. Rached, M. Driz, B. Bouhafs, Physica B 371 (2006) 12.
- [17] E. Tuncel, K. Colakoglu, E. Deligoz, Y.O. Ciftci, J. Phys. Chem. Solids 70 (2009) 371.
- [18] S. Yamaoka, O. Shimomura, H. Nakasawa, O. Fukunaga, Solid State Commun. 33 (1980) 87.
- [19] K. Mizushima, S. Yip, E. Kaxiras, Phys. Rev. B 50 (1994) 14952.
- [20] S. Zhang, N.-X. Chen, Modell. Simul. Mater. Eng. 11 (2003) 331.
- [21] S. Zhang, N.-X. Chen, Acta Mater. 51 (2003) 6151.